Emodin Prevented Depression in Chronic Unpredicted Mild Stress Exposured Rats by Targeting MiR139-5p/5-Lipoxygenase

Teng Zhang
Department of Pathology and Pathophysiology, School of Basic Medicine,Tongji Medical College, Huazhong University of Science and Technology; Department of Neurology, Shanxian Central Hospital, the Affiliated Huxi Hospital of Jining Medical College

Can Yang
Department of Pathology and Pathophysiology, School of Basic Medicine,Tongji Medical College, Huazhong University of Science and Technology

Jiang Chu
Departmrnt of Pathology and Pathophysiology, School of Basic Medicine,Tongji Medical College, Huazhong University of Science and Technology

Linna Ning
Department of Pathology and Pathophysiology, School of Basic Medicine,Tongji Medical College of Huazhong University of Science and Technology; Department of Pathology, Gannan Medical University Pingxiang Hospital

Peng Zeng
Department of Pathology and Pathophysiology, School of basic medicine, Tongji Medical College of Huazhong University of Science and Technology

Xiaoming Wang
Department of Pathology and Pathophysiology, Scool of Basic Medicine, Tongji Medical College, Huazhong University of Science and Technology

Yan Shi
Department of Pathology and Pathophysioloy, School of Basic Medicine, Tongji Medical College, Huazhong University of Science and Technology Department of Radiology

Baojian Qin
Department of Neuroloy, Shanxian Central Hospital, the Affiliated Huxi Hospital of Jining Medical College

Na Qu
Department of Pathology and Pathophysiology,School of Basic Medicine,Tongji Medical College of Huazhong University of Science and Technology; Department of Psychological Trauma, Affiliated Wuhan Mental Health Center, Tongji Medical College, Huazhong University of Science and Technology

Qi Zhang

Department of Psychiatry, Liyuan Hospital, Huazhong University of Science and Technology

Qing Tian (tianq@hust.edu.cn)

Tongji Medical College, Huazhong University of Science and Technology https://orcid.org/0000-0003-2795-363X

Research Article

Keywords: Emodin, Depression, miR139-5p, 5-lipoxygenase, Inflammation

Posted Date: March 10th, 2021

DOI: https://doi.org/10.21203/rs.3.rs-131425/v2

Abstract

Background: Using ingredients of medicinal plants is one of the goals of developing potential drugs for treating depression. Compelling evidences suggested anti-inflammation might block the occurrence of depression. Here, the effect of a natural compound, emodin, on the developing of psychosocial stress-induced depression and the underlying mechanism were studied.

Methods: 7 weeks' chronic unpredicted mild stress (CUMS) were performed to replicate psychosocial stress in rats, and sucrose preference test, force swimming test and open field test were used to evaluate their behaviors. The differentially expressed proteins in hippocampus were analyzed by proteomics. Nissl staining and Golgi staining were used to detect the losses of neurons and synapses, immunohistochemical staining was used to detect the activation of microglia, and ELISA was used to detect the levels of pro-inflammatory cytokines. Western blotting, immunofluorescence and quantitative PCR were also included.

Results: Hippocampal inflammation with up-regulated 5-lipoxygenase (5-LO) was observed in the depressed rats after CUMS exposure. And the up-regulation of 5-LO was proved to be caused by the decrease of miR139-5p. To observe the effect of emodin, we screened out depression susceptible (DeS) rats during CUMS and treated them with emodin (80mg/kg/day). 2 weeks later, emodin obviously prevented the depression behaviors of DeS rats and a series of pathological changes in their hippocampi, such as losses of neurons and spines, microglia activation, increased interleukin-1b and tumor necrosis factor-a, and the activation of 5-LO. Furtherly, we demonstrated that emodin inhibited its excess inflammatory responses possibly by targeting miR139-5p/5-LO and modulating the downstream glycogen synthase kinase 3β and nuclear factor erythroid 2-related factor 2.

Conclusions: These results provided an important evidence that emodin may be a candidate agent for the treatment of depression and established a key role of miR139-5p/5-LO in the inflammation of depression.

Introduction

Depression is a common psychiatric disease and one main cause of disability with a wide array of symptoms affecting somatic, cognitive, affective and social processes. It is characterized by low mood, sadness, insomnia, lack of interests in study, work and life, and so on. As a leading cause of global burden, the main treatments of depression are drug and psychological interventions[1, 2]. While effective, one third of people accepting drug intervention did not respond to these antidepressants, and others did not experience complete remission or relapsed due to numerous side effects of the chemical and synthetic drugs[3, 4]. Therefore, using ingredients of medicinal plants, which have many therapeutic benefits, is one of the goals of developing potential drugs for treating depression.

Psychosocial and environmental factors are the risk factors in the development of depression[5, 6], in which the important role of neuroinflammation has been highlighted by compelling clinical and preclinical evidences[7]. Clinic and rodents studies have shown that exposure to repeated psychosocial

and environmental stressors could cause considerable immunological alterations, including accumulation of pro-inflammatory cytokines and decrease of anti-inflammatory cytokines in the blood and brain[8-10]. As the major cellular component of the innate immune system in brain and the first line of defense, microglia play a critical role in neuroinflammation[11]. Activated microglia release pro-inflammatory cytokines, such as interleukin (IL)-1, IL-6, tumor necrosis factor-a (TNF-a) and nitric oxide (NO), and anti-inflammatory cytokines including IL-4 and IL-10. Acute psychological stressors in human have been identified continuously increase the circulating inflammatory factors[12]. In a Trier social stress test (TSST), the elevated levels of pro-inflammatory cytokines IL-6 and TNF-a were observed in healthy controls[13]. Chronic unpredicted mild stress (CUMS), an experimental method of replicating psychosocial and environmental stressors [14], has been shown cause hippocampal microglial activation [15, 16]. Activation of NOD-like receptor protein 3 (NLRP3) inflammasome and up-regulation of pro-inflammatory cytokines were observed in the hippocampus of depressed rats after CUMS [15, 16]. All these data suggested that neuroinflammation is an important mechanism linking psychosocial stress to depression.

Thus, targeting neuroinflammation has been recognized as a potential strategy for the prevention of psychosocial and environmental stressors induced depression. Some clinical trials have indicated better antidepressant effects for anti-inflammatory drugs, especially nonsteroidal anti-inflammatory drugs (NSAIDs) and cytokine-inhibitors[17]. However, some reported side effects have also raised controversy about whether NSAIDs can be used safely[17]. Emodin, a natural active compound extracted from a herb *rhubarb*, has the biological activity of anti-inflammation[18-20]. Therefore, we studied the effect of emodin on the depression-like behaviors of young male rats after CUMS exposure.

In this research, hippcampal neuroinflammation with the activation of 5-lipoxygenase (5-LO) in the development of depression was observed. To observe the effect of emodin, during 7 weeks' CUMS exposure we screened out the depression susceptible (DeS) rats and stress insensitive (Ins) rats at the end of 5^{th} week. Then, DeS rats received emodin treatment (Emo, 80mg/kg/day). 2 weeks later, emodin treated Des rats had their depression-like behaviors obviously improved. And a series of pathological changes in hippocampus, such as hippocampal neuron and spine loss, microglia activation, increased IL-1b and TNF-a and the activation of 5-LO have been revised by emodin. Additionally, we demonstrated that emodin inhibited its protections by targeting miR139-5p/5-LO.

Materials And Methods

Antibodies and Drugs

The primary antibodies used in this study are listed in Table 1. Emodin was obtained from Shanghai Base Industry (Shanghai, China) and dissolved in Tween-80, which was from Sinopharm Chemical Reagent Co., Ltd (Beijing, China). Anti-rabbit or anti-mouse IgG conjugated to IRDye@ (800CW) (1:10,000) was from Lincoln (USA). Toluidine blue and dimethyl sulfoxide (DMSO) were from Sigma (St. Louis, MO, USA). Diaminobenzidine (DAB) tetrachloride system was from Beijing Zhongshan Jinqiao BioteChinaology Co.,

Ltd. (Beijing, China). The miR139-5p inhibitor was from RiboBio Co.,Ltd. (Guangzhou, China). 3'-UTR of *5-LO* was amplified with the following primers: forward 5'-CGGGGTCTACAGTGCACGT-3', reverse 5'-CTCAACTGGTGTCGTGGAGTC -3'.

Cell Culture and Transfection

N2a cells were cultured with 45% DMEMhigh glucose medium and 45% Opti-MEM® I Reduced Serum Medium and supplemented with 10% fetal bovine serum (FBS), 100 U/ml penicillin, 0.1 mg/ml streptomycin (all from Hyclone) at 37°C in the presence of 5% CO_2. Transfection was performed with neofect (Neofect Biotechnology, Beijing, China) when cells were cultured to 70%~80% confluence in six-well plates. 48 hours after transfection, cells were collected and lysed for further research. HEK293 cells were cultured in high-glucose DMEM added with 10% FBS, 100 U/ml penicillin, 0.1 mg/ml streptomycin (all from Hyclone). Cells were incubated at 37 °C in a humidified atmosphere of 5% CO_2. HEK293 transfection was performed using Lipofectamine 2000 (Invitrogen, Carlsbad, California, USA).

Animals

8-week-old male Sprague-Dawley rats were supplied by Experimental Animal Central of Tongji Medical College, Huazhong University of Science and Technology (Wuhan, China). All efforts were made to minimize animal suffering and to reduce the number of rats used and all experimental procedures in this research have been approved by the Animal Care and Use Committee of Huazhong University of Science and Technology. Rats were housed 5 per cage in temperature controlled rooms (26 ± 2 °C) with standard rodent chow and water available ad libitum, keeping on a standard 12 hours light or dark cycle with the light on from 7:00 a.m. to 7:00 p.m. All rats were evaluated by Sucrose Preference Test (SPT), Forced Swimming Test (FST) and Open Field Test (OFT) before the expreiments. The behavioral tests were performed during the light cycle in a dedicated sound-proof behavioral facility by experimenters blind to treatment information. Rats were brought to the procedure room 1 hour before the start of behavioral test and remained in the same room through the test. At all times, the sound was masked with 60-65 dB white noises.

In the first part of this research (Fig. 1a), 45 rats were used, of which 15 rats were randomly chosen as control (Ctrl) rats, and 30 rats were daily exposed for 7 weeks' CUMS as reported[21, 22]. Depressed (Dep) rats were defined as those whose sucrose water intake decreased by more than 30% in SPT and their resting time increased by 50% during FST. Depression resistant (Res) rats were manifested as those having a greater sucrose water intake than the lower endpoint of the 95% confidence interval of that of control rats in SPT and a shorter immobility time than the upper endpoint of the 95% confidence interval of that of control rats in FST. After 7 weeks of CUMS exposure, 13 rats were in Res group and 14 rats were in Dep group, and the other 3 rats did not fit either group (Fig. 1a).

In the second part (Fig. 3a), we screened out depression susceptible rats (DeS) and stress insensitive rats (Ins) at the end of 5^{th} week during 7 weeks' CUMS exposure. A DeS rat was defined as who has a more than 20% decrease in sucrose water intake in SPT. An Ins rat should have a greater sucrose water intake

than the lower endpoint of the 95% confidence interval of that of control rats in SPT. In 64 CUMS exposed rats, 28 rats showed stress insensitive and 30 rats showed depression susceptible. Then, we treated control (Ctrl) and DeS rats with emodin (intragastric administration, 80mg/kg) or the same volume of solvent (Veh) daily (Fig. 3a). The dosage of emodin was referenced from previous studies[20, 23].

CUMS

The procedure of 7 weeks' CUMS exposure was performed as previously [21, 22]. Briefly, all stress-exposed rats were subjected to 3 or 4 following stressors each day, such as water or food deprivation for 24 hours, empty water bottles for 2 hours, cold room (4 °C) for 2 hours, hot room (45 °C) for 15 minutes, cage tilt for 16 hours, continuous overnight lighting for 12 hours, soiled cage (200 ml of water spilled onto the bedding) for 12 hours, grouped housing in one cage (4-5 per cage) for 12 hours, strobe lighting (200 flashes/minute) for 4 hours, intermittent white noise (85 dB) for 6 hours. The procedure was repeated for 7 weeks. The Ctrl rats were left undisturbed throughout with the exception of general handling (i.e., regular cage cleaning, water or food deprivation for SPT, and measuring body weight). Every week, SPT and weight weighing were performed.

SPT

SPT consists of 7 days of training phase, 24 hours of food and water deprivation phase, and 1 hour of testing phase. As previously, we trained the rat to consume 1.5% water sucrose solution for 1 hour (9:30 am-10:30 am) every day to adapt to novelty in the training phase. Then, the rat was deprived of food and water for 24 hours. In testing phase, rats were allowed free access to two pre-weighed bottles (containing water or 1.5% sucrose solution) for 1 hour. The sucrose preference was calculated as a percentage sucrose consumption × 100/ (water consumption + sucrose consumption).

OFT

The test was performed in a bare square box with 100 cm of length, 100 cm of width and 40 cm of height. As previously described[21], each rat were placed in the center of a black floor with 25 equal squares (20 cm × 20 cm square) including 16 peripheral squares and 9 central squares. The activity of rats was recorded by an overhanging camera linking to a computer over a 5 minutes' period. The number of total squares a rat crossing in the arena defined as the number of zones crossing was analyzed as measures of locomotor activity. The rearings were taken as measures of anxiety. The box was cleaned with 75% alcohol between tests.

FST

Next, rats were tested in a transparent plexiglas cylinders (20 cm of diameter, 50 cm of deepth, filled with 23-25 °C water to a depth of 25 cm) as previously[22]. As previously described [22], rats were individually forced to swim for 5 minutes. Each session was videotaped for analysis and the water was changed between sessions. The duration of immobility in 5 minutes was measured. The floating vertically in the water and making only those movements necessary to maintain the head above the surface of the water

for living were both considered as immobility. The immobility time was used for assessing feeling of hopelessness in rats.

Proteomic Analysis

The hippocampal proteomic analysis was conducted as previously described[21, 22, 24]. Briefly, the hippocampal proteins were extracted, digested and labeled by iTRAQ-6plex reagents in accordance with the manufacturer's protocol. Then, the peptides were fractionated by high pH reverse-phase HPLC. The resulting fractions were dissolved, loaded onto a reversed-phase pre-column (Acclaim PepMap 100, Thermo Scientific), and then separated by a reversed-phase analytical column (Acclaim PepMap RSLC, Thermo Scientific). The peptides were accepted to NSI source followed by tandem mass spectrometry (MS/MS) in Q Exactive^{TM} Plus (Thermo) coupled online to the UPLC. In order to identify the proteins, we analyzed the resulting MS/MS data using Mascot search engine (v.2.3.0) and searched against Uniprot_rat database (32,983 sequences). We defined the proteins with iTRAQ ratios of >1.15 or <0.87 coupled with p <0.05 as differentially expressed proteins. Interaction network of differentially expressed proteins were made by STRING 11.0.

Morphological Techniques on Brain Slices

Rats were anesthetized with isoflurane and transcardially perfused with 100 milliliters normal saline and then perfused with 400 milliliters 4% paraformaldehyde solution. The brain was removed from the skull carefully. For Nissl staining, immunohistochemical staining and immunofluorescence staining, the brain was post-fixed in 4% paraformaldehyde solution for another 24 hours at 4 °C. In the dehydration, the sample was subjected to 20% and 30% sucrose gradient dehydration for twice until completely sunken. All brains were sliced into 30 μm coronal sections with a freezing microtom (Kryostat 1720, Leitz, Wetzler, Germany). The sections were consecutively collected and stored in 50% glycerinum in PBS at -20 °C.

Nissl Staining

The sections were washed with PBS for 2 minutes ´ 3 times, pasted on the slides and air-dried for 2 hours. Then they were immersed into Nissl dye liquor for several minutes according to the color changing, followed by decoloration in 75% alcohol, 95% alcohol twice for several minutes each. Subsequently, use the absolute ethyl alcohol for dehydration for 5 minutes ´ 3 times and the dimethylbenzene for transparency for 10 minutes twice. The sections were sealed and dried in fume hood. The images were obtained by an optical microscope (Nikon 90i, Tokyo, Japan).

Immunohistochemical and Immunofluorescence Staining

After being washed with PBS for 5 minutes ´ 3 times and treated by PBS containing 0.3% H_2O_2 and 0.5% Triton X-100 for 30 minutes at room temperature, the sections were pre-incubated with 3% normal goat serum and incubated in the primary antibodies (Table 1). 24 hours later, they were incubated for 1 hour with the secondary antibodies (Table 1) for 1 hour at 37°C after being washed with PBS. For

immunohistochemical staining, immunoreaction was developed using Histostain TM-SP kits (ZSGB-Bio, Beijing, China) and visualized with diaminobenzidine (brown). The images were obtained by an optical microscope (Nikon 90i, Tokyo, Japan). For immunofluorescence stained sections, the images were observed using a laser scanning confocal microscope (Zeiss LSM 710, Germany).

Golgi Staining

After the brain was removed from the skull, golgi staining was developed using the FD Rapid GolgiStain kit (FD Neurotechnologies, Baltimore, MD) according to the manufacturer's protocol. The samples were cut into horizontal sections of 100 μm thicknesses using a vibratome (Leica, Nussloch, Germany; S100, TPI) and mounted on the gelatin-coated slide. The sections were dehydrated in successive alcohol and transparency in xylene, and then the slide was sealed. The sections were observed and imaged by using an ordinary optical microscope (Nikon 90i, Tokyo, Japan). The number of dendritic spines on hippocampus pyramidal neurons was counted in Image-Pro Plus 6.0 software (Media Cybernetics, Inc. USA).

Western Blotting

The rats were anaesthetized with isoflurane and sacrificed. The hippocampi were quickly dissected out of brain and frozen at -80 °C. For the analysis of whole cell components, the sample of hippocampus was homogenized in cold buffer solution containing 10 mM Tris-HCl (pH 7.4), 50 mM NaCl, 50 mM NaF, 0.5 mM Na_3VO_4, 1 mM EDTA, 1 mM benzamidine, 1.0 mM phenylmethylsulfonyl fluoride (PMSF), 5 mg/ml leupeptin, 5 mg/ml aprotinin and 2 mg/ml pepstatin. Lysates were mixed with 4 × extracting buffer and protein concentrations were determined using a BCA protein assay kit (Rockford, IL, USA). All the sample solutions were stored at -80 °C for use. For Western blotting analysis of nuclear and cytoplasmic fractions[25], proteins were extracted with the kit from KeyGen Biotech (NanJing KeyGen Biotech Co.,Ltd.).

Before sample-loading, a final concentration of 10% β-mercaptoethanol and 0.05% bromophenol blue were added. The proteins were separated by 10% sodium dodecyl sulfate polyacrylamide gel electrophoresis (SDS-PAGE) and probed with primary antibodies (Table 1). Secondary antibodies were anti-rabbit or anti-mouse IgG conjugated to IRDye@ (800 CW; 1:10,000). The intensities of immunoblotting strips were automatically recognized by the Odyssey system (Li-Cor Bioscience, Lincoln, Nebraska, USA). All intensities of strips were normalized by the average intensity of DM1A. Then take the average value of Ctrl group as 1, and calculate the relative intensity of each strip.

Quantitative Real-time Polymerase Chain Reaction (qPCR)

Total RNA was extracted from hippocampal using TRIzol reagent (Invitrogen, Carlsbad, California, USA) according to the manufacturer's protocol. $RNA_{260/280}$ was measured spectrophotometrically for determining the concentration and purity. To synthesise cDNA from miRNA, we used M-MLV Reverse Transcriptase cDNA Synthesis Kit (Invitrogen, Carlsbad, California, USA) according to the supplier's

recommendations. The qPCR amplifcation was performed by CFX96 Real-Time PCR Detection System (Bio-Rad, Hercules, California, USA) and SYBR Green Premix Ex TaqTM (TaKaRa, Kyogo, Japan). The reaction conditions were as follows, an initial denaturation 3 minutes at 95 °C, followed by 45 cycles 10 seconds at 95 °C, 30 seconds at 60 °C, and extension 30 seconds at 72 °C. The primers for qPCR analysis were designed and synthesized. The data was quantified using the ΔΔCt-method.

Luciferase Assays for Identifying miR-target Interactions

Normal and mutated 3'-UTR sequences of *5-LO* were subcloned into the psiCHECK-2 reporter plasmid (Qijing Biotechnology Co., Ltd., Wuhan, China) as previously described[26]. HEK293T cells were transfected with psiCHECK-2 plasmid containing the 3'-UTR and the overexpressing vector for a specific miRNA. 24 hours after transfection, cells were lysed and luciferase reporter activities were assayed as previously described[26].

Enzyme-linked Immuno Sorbent Assay (ELISA)

The hippocampal levels of IL-1b, TNF-α and leukotriene B4 (LTB4) were assayed by ELISA according to the protocols of ELISA kits (Elabscience Biotechnology Co., Ltd, Wuhan, China). A microplate reader (Biotek, Winooski, VT, USA) set to 450 nm was used to determine the optical density (OD) of value. A standard curve was created by plotting the mean OD value for each standard. The sample concentration was determined from the standard curve.

Predictions of microRNA Targeting

The miR-targeting predictions were performed by 3 different web-based algorithms, Targetscan software (http://www.targetscan.org), miRbase (http://www.mirbase.org/), and miRDB (http://www.mirdb.org/miRDB/).

Statistical Analysis

The data were analyzed using SPSS 12.0 (SPSS Inc., Chicago, Illinois, USA) and the statistical graphs were produced by GraphPad Prism (GraphPad Software, Inc., La Jolla, CA). Data were expressed as means ± SEM.. Differences among groups were tested with the one-way analysis of variance (ANOVA) procedure. The level of significance was set at $p < 0.05$.

Results

Inflammation with increased 5-LO was found in hippocampus of Dep rats

Before CUMS exposure, all the rats (n=45) have identical rate of preference to sucrose (about 85%) in SPT, equivalent immobility time (about 79.3 seconds) in FST, and equivalent number of zone crossing (about 154) and rearing times (about 27) in OFT. After 7 weeks' CUMS exposure, 13 Res rats and 14 Dep rats were obtained (Fig. 1a). The Dep rats showed a robust decrease (45.1%) in sucrose intake, whereas

Res rats displayed a sucrose preference (83.2%) similar to that of unstressed Ctrl rats (Fig. 1b). In FST, the Dep rats had a much longer immobility time (220 ± 4.4 seconds) than Res rats (83.3 ± 5.8 seconds) and Ctrl rats (78.1 ± 5.3 seconds) (Fig. 1c). In OFT, the number of zone crossing and rearing times of Dep rats were less than those of Res rats and Ctrl rats (Fig. 1d, e). Additionally, we found both Dep (354.1 ± 6.4 g) and Res (353.5 ± 9.5 g) rats had lighter body weights than Ctrl rats (471.1 ± 5.8 g) (Fig. 1f).

In the proteomics data with 3645 quantified proteins, 262 differentially expressed proteins were obtained, including 40 up-regulated and 53 down-regulated differentially expressed proteins in Dep/Ctrl, 75 up-regulated and 34 down-regulated differentially expressed proteins in Dep/Res, and 40 up-regulated and 101 down-regulated differentially expressed proteins in Res/Ctrl (fig. 1g). The protein-protein interaction (PPI) network analysis suggested inflammation was the characteristic signal in hippocampus of Dep rats (Fig.1h, i). Fibrinogen (Fg) is the acute phase protein and a marker of inflammation[27]. Increased Fg was reported contribute to nuclear factor-κB (NF-κB) activation[27]. Up-regulated Fga, Fgb and Fgg levels in whole blood samples were found in depressed patients[28]. Filamin A (Flna) was reported associated with toll-like receptor-4 (TLR4), the innate immune receptor responsible for inflammatory cytokine release[29]. a2-HS glycoprotein (Ahsg, also known as fetuin-A), an endogenous ligand for TLR4, was reported involved in lipid-induced inflammation by activating NF-κB[30, 31]. Elevated serum Ahsg was reported in male patients with major depressive disorder (MDD)[32]. Increased Fga, Fgb, Fgg and Ahsg were shown in Dep/Ctrl and Dep/Res, but not Res/Ctrl (Fig.1j). Additionally, increased vimentin (Vim)[33], collagen type I α 1 chain (Col1a1)[34], annexin A1 (Anxa1)[35] , Anxa2[36] and Galectin-1 (Gal-1, lgals1) [37] indicated the elevated inflammatory responses to CUMS and/or increased the permeability of blood-brain barrier (BBB) in hippocampus[33] (Fig.1j). Astrocytic glutamate transporter-1 (GLT1, slc1a2) is responsible for up to 95% of extracellular glutamate clearance, and several lines of evidence suggest that it is essential for brain functioning[38]. The pro-inflammatory cytokines led to a significant down-regulation of GLT1 in astrocyte[39]. Furtherly, by ELISA we found that the levels of IL-1β and TNF-α in the hippocampus of Dep rats were more than twice as high as those in Res and Ctrl rats (Fig.1m, n). In PPI network analysis (Fig.1h, i), 5-LO (ALOX5) has more connections with the differentially expressed proteins in Dep/Ctrl and Dep/Res. By Western blotting, 5-LO level in hippocampus of Dep rats was shown much higher than those in Res and Ctrl rats (Fig.1k, l). All these data indicated the important role of hippocampal neuroinflammation with up-regulated 5-LO in depression.

Reduction of miR139-5p induced 5-LO elevation

Although 5-LO plays a key role in neuroinflammation [40-42], its regulation is still not fully understood. By Targetscan software (http://www.targetscan.org), miRbase (http://www.mirbase.org/), and miRDB (http://www.mirdb.org/miRDB/), we found that miR139-5p and miR7a were scored the highest in both predicted outputs. By qPCR, the hippocampal level of miR139-5p was found dramatically decreased in Dep rats (Fig. 2a). To verify the posttranscriptional regulation of 5-LO by miR139-5p, we constructed the wild-type 3'-UTR of 5-*LO* (*ALOX5* Wt, containing the binding site to miR139-5p) and a mutated version (*ALOX5* Mut) to the luciferase reporter vector, which were cotransfected into HEK293 cells with miR139-5p mimic or a negative control (miR-mimic NC) (Fig. 2b). Overexpression of miR139-5p suppressed the

expression of the luciferase reporter gene with the *5-LO* 3'-UTR, whereas the expression of reporter was not suppressed when we mutated the miR139-5p recognition site located on the *5-LO* 3' UTR (Fig. 2c). Moreover, the miR139-5p inhibitor elevated the protein level of 5-LO in N2a cells (Fig. 2d, e). These results showed that miR139-5p inhibited 5-LO expression at a posttranscriptional level, while the loss of miR139-5p mediated 5-LO elevation in depression.

Emodin ameliorates depressive-like behaviors in DeS rats

Emodin was reported as an inhibitor of 5-LO[43]. Then, we investigated whether emodin could prevent the develepent of depression in rats exposed to CUMS. In the first part of research (Fig. 1a), the success rate of depression replication in rats by 7 weeks' CUMS was 46.67%. Therefore, we selected out 30 depression-susceptible rats (DeS rats) and 28 stress insensitive rats (Ins rats) from 64 rats at the end of 5^{th} week during 7 weeks' CUMS exposure. Those DeS rats showed a significantly lower sucrose preference rate (61.6%) than stress insensitive rats (85.3%) and control rats (86.5%) (Fig. 3b). Then, 30 DeS rats and 30 Ctrl rats received daily emodin treatment (Emo, 80mg/kg) or the same volume of solvent treatment (Veh) for 2 weeks (Fig. 3a). Meanwhile, DeS rats were exposed to CUMS continuously. 2 weeks later, DeS+Veh rats (body weight 355.7 ± 5.0 g) presented depressive behaviors, e.g. a lower sucrose preference (44.1%) in SPT (Fig. 3c) and an obvious longer immobility time (210.2 ± 3.4 seconds) in FST (Fig. 3d). However, DeS+Emo rats had a higher percent of sucrose preference (78.5%) in SPT (Fig. 3c) and a much shorter immobility time (78.5 ± 5.0 seconds) in FST (Fig. 3d), much more crossing zones and rearing times in OFT (Fig. 3e, f), and an increased body weight (435.6 ± 2.9 g, Fig. 3g) than DeS+Veh rats. Emodin treatment had no effects on the emotional behaviors and body weight of Ctrl rats.

Studies in humans and animals have confirmed the reduced volume of the hippocampus in depressed brain, which was characterized by loss of neurons and loss of synapses [44, 45]. In this research, by Nissl staining we found DeS+Veh rats had much less neurons in hippocampal CA1, CA3 and DG regions (Fig. 3h-k), whereas no obvious hippocampal neuron loss was observed in DeS+Emo rats (Fig. 3h-k). By Golgi staining, DeS+Veh rats showed the significant decreased density of dendritic spines and number of mushroom-type spines in CA1 (Fig. 3l-n). DeS+Emo rats had more sipnes, especially mushroom-type spines, than DeS+Veh rats (Fig. 3l-n). Similar alterations of dendritic spines in CA3 and DG were observed (data not shown). Emodin treatment had no effects on the hippocampal neuron number and spine density of Ctrl rats.

All these data suggested that emodin prevented the depression-like behaviors and ameliorated the losses of hippocampal neuron and dendritic spine in depressed brain.

Emodin inhibited the activation of 5-LO by up-regulating miR-139-5p

5-LO, an important pro-inflammatory enzyme widely expressed in brain, initiates leukotrienes (LTs) synthesis from arachidonic acid. DeS+Veh rats had higher levels of 5-LO and LTB4 (a major metabolic product of 5-LO activation) than DeS+Emo rats and Ctrl+Veh rats (Fig. 4a-c). Emodin did not change the levels of 5-LO and LTB4 in Ctrl rats (Fig. 4a-c). Upon stimulation, 5-LO could be translated to nuclear and

perinuclear membranes, and this translocation is regarded as a determinant of its LTB4 synthetic capacity[46]. Therefore, the homogenate of hippocampus was divided into cytoplasmic and nuclear fractions. It was found that DeS+Veh rats, but not DeS+Emo rats, had the significantly higher nuclear 5-LO level than Ctrl+Veh and Ctrl+Emo rats (Fig. 4e, f). By immunofluorescence staining and fluorescence intensity distribution analysis (FIDA) in neurons of CA1 (Fig. 4h-j), CA3 and DG (data not shown), more 5-LO was observed in the nucleus in DeS+Veh rats, whereas it was mainly in the cytoplasm in DeS+Emo (Fig. 4h-j) and Ctrl rats (data not shown).

5-LO inhibition might down-regulate NF-κB[40, 47]. NF-κB, consisting of p50 and p65, resides in the cytoplasm of resting cells. In response to stimulation, NF-κB p65 is activated and translocates to the nucleus, followed by binding to specific DNA sequences in target genes involved in inflammation and apoptosis [47, 48]. In this research, increased NF-κB p65 was found in hippocampui of DeS+Veh rats (Fig. 4a, d), and this increasing was mainly concentrated in the nuclear fraction (Fig. 4e, g). Emodin treatment significantly prevented the increasing nuclear NF-κB p65 (Fig. 4e, g). We also found hippocampal miR139-5p was significantly decreased in DeS+Veh rats (Fig. 4k), whereas no obvious decreasing of miR139-5p was shown in DeS+Emo rats (Fig. 4k). These results suggested that emodin inhibit the activation of 5-LO partially by up-regulating miR139-5p.

Depression associated microglia activation was inhibited by emodin

Microglia is found associated with inflammation in depression [49, 50]. By Iba1 (a microglial marker)-based immunohistochemical staining (Fig. 5a), the obvious increased densities of microglia in hippocampal CA1, CA3 and DG regions of DeS+Veh rats were found. The densities of microglia in DeS+Emo rats were significant decreased compared with DeS+Veh rats (Fig. 5a-d). Increased solidity (the ratio between the positive area and the convex area) represents the activation of microglia[23, 51, 52]. In this research, we divided the solidity value of the microglia into 3 grades, e.g. <0.25 (ramified), 0.25-0.31 (hypertrophied) and >0.31 (bushy, also termed as amoeboid), and the higher solidity value indicates higher activation of microglia[51]. As shown in Figure 5e and f, 69% microglia in Ctrl+Veh rats, 67.1% in Ctrl+Emo rats and 56.6% in DeS+Emo rats had their solidity value below 0.25. Only 16.4% microglia in DeS+Veh rats had their solidity value below 0.25. DeS+Veh rats had the most microglia (48.4%) with the highest solidity value, greater than 0.31, indicating their activation. By ELISA, DeS+Veh rats had the obvious increased levels of IL-1β and TNF-α in their hippocampi (Fig. 5g, h). There was no difference in the proportion of microglia solidity value and levels of IL-1β and TNF-α between DeS+Emo and Ctrl rats. All these data suggested that the depression associated microglia activation was inhibited by emodin.

Emodin inhibited hippocampal glycogen synthase kinase 3β(GSK3β) activation

GSK3β is suggested to be engaged in the pathogenesis of depression, and to be a target and/or modifier of anti-depressants' action[53]. Previous research suggested stress leads to GSK3β activation depending on 5-LO[54]. In this research, the total levels of hippocampal GSK3β were equal in all groups, while its phosphorylation level at Ser9 (p-GSK3β, inactive form) was significantly decreased in DeS+Veh rats (Fig. 6a, b). Furthermore, the decreasing of phosphorylated GSK3β at Ser9 was observed in both cytoplasmic

and nuclear fractions of DeS+Veh rats (Fig. 6c, d). In hippocampi of DeS+Emo rats, the phosphorylation levels of GSK3β at Ser9 in both cytoplasmic and nuclear fractions were higher than those in DeS+Veh rats, indicating the inhibition of emodin on GSK3β activation (Fig. 6c, d). Furtherly, we detected the levels of nuclear factor erythroid 2-related factor 2 (Nrf2), which is a transcriptional activator of antioxidant genes and down-regulated in depression[55]. GSK3β could indirectly phosphorylate Nrf2 (at Tyr568) [56, 57] or directly phosphorylate Nrf2 (at Ser335 and Ser338), resulting in nuclear export and cytoplasmic degradation of Nrf2[58]. We observed decreased nuclear Nrf2 and increased cytoplasmic Nrf2 in hippocampi of DeS+Veh rats, indicating the increased the nuclear export of Nrf2 (Fig. 6e, f). In hippocampi of DeS+Emo rats, the nuclear export of Nrf2 was not observed (Fig. 6e, f). Additionally, decreased phosphorylation of Nrf2 at Ser40 was observed in the nuclear fraction of DeS+Veh rats (Fig. 6e, f). The phosphorylation of Nrf2 at Ser40 is important for its transcriptional property. DeS+Emo rats had much more nuclear Ser40 phosphorylated Nrf2 than the other three groups of rats (Fig. 6e, f). The alterations of phosphorylated Nrf2 at Ser40 were confirmed by its immunohistochemical and immunofluorescence staining in brain slices (Fig. 6g, h). All these data suggested that emodin inhibits GSK3β activation and may act as an Nrf2 activator.

Discussion

In this research, emodin, a natural compound with anti-5-LO activity, blocked the occurrence of stress-induced depression. The significantly up-regulated hippocampal differentially expressed proteins, e.g. Fga, Fgb, Fgg, Ahsg, Col1a1 and Anxa2, suggested hippocampal inflammation in the development of depression, which was confirmed by the activated microglia and the increased IL-1b, TNF-a and NF-κB p65 in hippocampi of depressed rats. Increased hippocampal 5-LO and its major metabolic product LTB4 suggested the activation of 5-LO. Emodin obviously prevented the depression behaviors and a series of pathological changes of hippocampus, such as hippocampal neuron and spine loss, microglia activation, increased IL-1b and TNF-a, and the activation of 5-LO and GSK3β. Furthermore, we demonstrated that emodin blocked 5-LO related inflammation by targeting miR139-5p. Thus, our study also uncovered a novel role for miR139-5p and 5-LO in the pathogenesis of depression.

Psychosocial stress is one of the leading factors for development of depression. When exposed to the same stress conditions, some individuals do not show depressive symptoms, which are called depression resistance. Understanding the mechanism of depression resistance is helpful to prevent the occurrence of depression. In this study, 43.3% of the rats showed significant depression resistance, while 46.67% of the rats developed depression after 7 weeks' CUMS exposure. Although previous studies have reported different pathophysiological characteristics between depression and depression resistant animals [54, 56], our results highlight that 5-LO activation associated hippocampal inflammation is the key pathological process. When CUMS exposed, rats presented depression as long as inflammation occurred in their hippocampi. While the inflammation did not occur or was inhibited, the rats showed depression resistance. miR139-5p, a neuron enriched miRNA in brain, was found markedly suppressed in hippocampus of depressed rats. It has been demonstrated to attenuate brain damage through regulating neuronal apoptosis and mediating behavioral responses to chronic stress in rats[59, 60]. Here, we showed

that miR139-5p specifically binds to the 3'-UTR of *5-LO* and represses 5-LO expression. And emodin prevented a decrease of miR139-5p and an increase of 5-LO, and effectively ameliorated hippocampal NF-κB p65 up-regulation, increasing of pro-inflammatory factors and microglia activation in depression rats. These findings strongly suggest the critical roles of miR139-5p and 5-LO in the pathogenesis of psychosocial stress induced neuroinflammaion.

Activated GSK-3β was reported in brains of depression, and GSK-3β inhibition was a therapeutic target of depression[61, 62]. Although 5-LO has been revealed to be involved in stress-induced activation of GSK3β[63], the underlying mechanism is still unclear. In this study, GSK3β activation was shown in hippocampi of DeS+Veh rats by decreased phosphorylation levels of GSK3β at Ser-9. When 5-LO was down-regulated after emodin treatment, GSK3β activity was partially restored. The phosphorylation of GSK3β at Ser-9 is regulated by phosphoinositide 3-kinase/protein kinase B (PI3K/AKT), mitogen-activated protein kinase/extracellular signal-regulated kinase (MAPK/ERK), protein kinase A (PKA), integrin-linked kinase (ILK), calcium/calmodulin dependent protein kinase 2 (CaMK2) and WNT signaling[53]. On the other hand, dephosphorylation of Ser-9 by protein phosphatase 1 (PP1), PP2A and PP2B directly activates GSK3β[53]. Further exploring how 5-LO activates GSK3β is of great significance to understand the key role of inflammation in the occurrence of depression.

Nrf2, a transcription factor, plays a central role in regulating inflammation and regulating production of antioxidants and antioxidant enzymes [64-66]. It was reported that ablation of Nrf2 triggers depression-like behaviors related to an increased inflammation and Nrf2 agonist afforded antidepressant-like effects in an animal inflammatory model of depression[67]. Under basal conditions, Keap-1 maintains Nrf2 in the cytoplasm by forming Keap1-Nrf2 complex, and then Nrf2 is ubiquitinated and subsequently degraded by the 26S proteasome[68]. When a moderate stimulus appears, Nrf2 is more phosphorylated at Ser40 and transferred to the nucleus, and then play a protective role[69, 70]. Here, in DeS+Veh rats, the increased nuclear export of Nrf2 and decreased phosphorylation of nuclear Nrf2 at Ser40 was observed. GSK3β could indirectly phosphorylate Nrf2 (at Tyr568) by activating src-related kinase Fyn[56, 57] or directly phosphorylate Nrf2 (at Ser335 and Ser338), resulting in nuclear export and cytoplasmic degradation of Nrf2[58]. Thus, the increased nuclear export of Nrf2 in hippocampus of depressed rats might be caused by GSK3β activation. The mechanism for the decreased phosphorylation of nuclear Nrf2 at Ser40 needs further investigations.

Emodin was reported to act as an inhibitor of 5-LO[43] and inhibit lipopolysaccharide (LPS) induced microglial activation, as well as protect synaptic transmission of hippocampal neurons from glutamate excitotoxicity[71, 72]. Whether emodin could cross the blood brain barrier is not known. A recent study[73] and the proteomic data in this research showed the hippocampal BBB disruption, which promotes emodin to enter hippocampus conveniently. Additionally, CUMS has been shown to generate inflammation in the liver and pancreas of rats[74] and vascular inflammation in rabbits[75]. Emodin may also antagonize the systemic inflammation induced by CUMS, which needs further experimental confirmation. Our findings are consistent with previous studies where it was found that pharmacological inhibition 5-LO ameliorates depression-like behaviors or cognitive impairment[76, 77]. In our study, CUMS

induced the activation of 5-LO in DeS+Veh rats. Although the elevated 5-LO was not restored to a normal level in DeS+Emo rats, the emodin-treatd DeS rats had a normal activity of 5-LO.
Previous research suggested that stress led to an elevation of 5-LO activity due to the level and translocation of 5-LO[78, 79]. By further study, the 5-LO in the nucleus was found to significantly increase in DeS+Veh rats, while emodin treated DeS rats had an evaluated 5-LO in the cytoplasm other than in the nucleus. As mentioned above, decreased miR139-5p level in DeS+Veh rats was rescued by emodin. These findings indicated that emodin not only decreased 5-LO level by acting on miR139-5p, but also decreased 5-LO activity by inhibiting its nuclear translocation.

Conclusions

Taken together, this study demonstrated emodin blocked the occurrence of CUMS induced depression by inhibiting 5-LO related inflammation via up-regualting miR139-5p. These results established a key role of miR139-5p/5-LO in the development of stress-induced depression and provided an important evidence that emodin may be a candidate agent for the treatment of depression (Fig. 7).

Declarations

Acknowledgements

Not applicable.

Authors' contributions

Zhang Teng and Yang Can conceived and directed the study, interpreted the results, and wrote the manuscript. Zhang Teng and Tian Qing designed and performed most of the experiments and analyzed most of the results. Chu Jiang, Ning Linna, Zeng Peng, Wang Xiaoming, Shi Yan, and Qin Baojian contributed to the experiments. Qu Na and Zhang Qi provided supervision. Zhang Teng, Ning Linna, Qu Na, and Tian Qing provided funding for experiments. The authors read and approved the final manuscript.

Funding

This work was supported by grants from the Natural Science Foundation of China (82071478, 81960260), the Natural Science Foundation of Shandong Province (ZR2020QH129), the Natural Science Foundation of Hubei Province (2020CFB857) and Supporting Fund for Teachers' research of Jining Medical University (JYFC2019FKJ034).

Availability of data and materials

The datasets and materials used and/or analyzed during current study are available from the corresponding author on reasonable request.

Ethics approval and consent to participate

All experimental protocols were approved by the Animal Care and Use Committee of Huazhong University of Science and Technology.

Consent for publication

Not applicable.

Competinginterests

The authors declared no potential conflicts of interest with respect to the research, authorship, and/or publication of this article.

Authors'information

[1]Department of Pathology and Pathophysiology, School of Basic Medicine, Tongji Medical College; Key Laboratory of Neurological Disease of National Education Ministry, Huazhong University of Science and Technology, Wuhan 430030, China

[2]Department of Neurology, Shanxian Central Hospital, the Affiliated Huxi Hospital of Jining Medical College, Heze 274300, China

[3]Department of Pathology, Gannan Medical University Pingxiang Hospital, Pingxiang 337055, China

[4]Department of Psychological Trauma, Affiliated Wuhan Mental Health Center, Tongji Medical College, Huazhong University of Science and Technology, Wuhan 430022, China

[5]Research Center for Psychological and Health Sciences, China University of Geosciences, Wuhan 430074, China

[6]Department of psychiatry, Liyuan Hospital, Huazhong University of Science and Technology, Wuhan 430077, China

Abbreviations

Dep: Depression; Res: Depression resistant; Ctrl: Control; CUMS: Chronic unpredicted mild stress; DeS: Depression susceptible; Ins: Stress insensitive; Emo: Emodin; Veh: Vehicle; IL: Interleukin; TNF-a: Tumor necrosis factor-a; 5-LO: 5-lipoxygenase; GSK3β: Glycogen synthase kinase 3β; Nrf2: Nuclear factor erythroid 2-related factor 2; NF-κB: Nuclear factor-κB; TSST: Trier social stress test; NO: Nitric oxide; NLRP3: NOD-like receptor protein 3; NSAIDs: Nonsteroidal anti-inflammatory drugs; SPT: Sucrose preference test; FST: Force swimming test; OFT: Open field test; PMSF: Phenylmethylsulfonyl fluoride; LTB4: Leukotriene B4; OD: Optical density; PPI: Protein-protein interaction; MDD: Major depressive disorder; Fg: Fibrinogen; Ahsg: a2-HS glycoprotein; Vim: Vimentin; TLR4:Toll-like receptor-4; Col1a1:

Collagen type I α 1 chain; Anxa1: Annexin A1; BBB: Blood-brain barrier; GSTA4: Glutathione S-transferase A4; LPS: Lipopolysaccharide.

References

1. Smith K. Mental health: a world of depression. Nature 2014; 515(7526):181.
2. Murray CJ, Atkinson C, Bhalla K, Birbeck G, Burstein R, Chou D, et al. The state of US health, 1990-2010: burden of diseases, injuries, and risk factors. JAMA 2013; 310(6):591-608.
3. Rush AJ, Trivedi MH, Wisniewski SR, Nierenberg AA, Stewart JW, Warden D, et al. Acute and longer-term outcomes in depressed outpatients requiring one or several treatment steps: a STAR*D report. Am J Psychiatry 2006; 163(11):1905-17.
4. Shelton RC, Osuntokun O, Heinloth AN, Corya SA. Therapeutic options for treatment-resistant depression. CNS Drugs 2010; 24(2):131-61.
5. Hodes GE, Kana V, Menard C, Merad M, Russo SJ. Neuroimmune mechanisms of depression. Nat Neurosci 2015; 18(10):1386-93.
6. Wohleb ES, Franklin T, Iwata M, Duman RS. Integrating neuroimmune systems in the neurobiology of depression. Nat Rev Neurosci 2016; 17(8):497-511.
7. Troubat R, Barone P, Leman S, Desmidt T, Cressant A, Atanasova B, et al. Neuroinflammation and depression: A review. Eur J Neurosci 2021; 53(1):151-171.
8. Howren MB, Lamkin DM, Suls J. Associations of depression with C-reactive protein, IL-1, and IL-6: a meta-analysis. Psychosom Med 2009; 71(2):171-86.
9. Kim YK, Na KS, Myint AM, Leonard BE. The role of pro-inflammatory cytokines in neuroinflammation, neurogenesis and the neuroendocrine system in major depression. Prog Neuropsychopharmacol Biol Psychiatry 2016; 64:277-84.
10. Muller N, Schwarz MJ, Dehning S, Douhe A, Cerovecki A, Goldstein-Muller B, et al. The cyclooxygenase-2 inhibitor celecoxib has therapeutic effects in major depression: results of a double-blind, randomized, placebo controlled, add-on pilot study to reboxetine. Mol Psychiatry 2006; 11(7):680-4.
11. Prinz M, Jung S, Priller J. Microglia Biology: One Century of Evolving Concepts. Cell 2019; 179(2):292-311.
12. Steptoe A, Hamer M, Chida Y. The effects of acute psychological stress on circulating inflammatory factors in humans: a review and meta-analysis. Brain Behav Immun 2007; 21(7):901-12.
13. Gaab J, Rohleder N, Heitz V, Engert V, Schad T, Schurmeyer TH, et al. Stress-induced changes in LPS-induced pro-inflammatory cytokine production in chronic fatigue syndrome. Psychoneuroendocrinology 2005; 30(2):188-98.
14. Willner P. Validity, reliability and utility of the chronic mild stress model of depression: a 10-year review and evaluation. Psychopharmacology (Berl) 1997; 134(4):319-29.

15. Yue N, Huang H, Zhu X, Han Q, Wang Y, Li B, et al. Activation of P2X7 receptor and NLRP3 inflammasome assembly in hippocampal glial cells mediates chronic stress-induced depressive-like behaviors. J Neuroinflammation 2017; 14(1):102.
16. Wang YL, Han QQ, Gong WQ, Pan DH, Wang LZ, Hu W, et al. Microglial activation mediates chronic mild stress-induced depressive- and anxiety-like behavior in adult rats. J Neuroinflammation 2018; 15(1):21.
17. Kohler O, Krogh J, Mors O, Benros ME. Inflammation in Depression and the Potential for Anti-Inflammatory Treatment. Curr Neuropharmacol 2016; 14(7):732-42.
18. Dong X, Fu J, Yin X, Cao S, Li X, Lin L, et al. Emodin: A Review of its Pharmacology, Toxicity and Pharmacokinetics. Phytother Res 2016; 30(8):1207-18.
19. Huang HC, Chang JH, Tung SF, Wu RT, Foegh ML, Chu SH. Immunosuppressive effect of emodin, a free radical generator. Eur J Pharmacol 1992; 211(3):359-64.
20. Li M, Fu Q, Li Y, Li S, Xue J, Ma S. Emodin opposes chronic unpredictable mild stress induced depressive-like behavior in mice by upregulating the levels of hippocampal glucocorticoid receptor and brain-derived neurotrophic factor. Fitoterapia 2014; 98:1-10.
21. Ning LN, Zhang T, Chu J, Qu N, Lin L, Fang YY, et al. Gender-Related Hippocampal Proteomics Study from Young Rats After Chronic Unpredicted Mild Stress Exposure. Mol Neurobiol 2018; 55(1):835-850.
22. Qu N, Wang XM, Zhang T, Zhang SF, Li Y, Cao FY, et al. Estrogen Receptor alpha Agonist is Beneficial for Young Female Rats Against Chronic Unpredicted Mild Stress-Induced Depressive Behavior and Cognitive Deficits. J Alzheimers Dis 2020; 77(3):1077-1093.
23. Zeng P, Shi Y, Wang XM, Lin L, Du YJ, Tang N, et al. Emodin Rescued Hyperhomocysteinemia-Induced Dementia and Alzheimer's Disease-Like Features in Rats. The international journal of neuropsychopharmacology 2019; 22(1):57-70.
24. Fang YY, Zeng P, Qu N, Ning LN, Chu J, Zhang T, et al. Evidence of altered depression and dementia-related proteins in the brains of young rats after ovariectomy. J Neurochem 2018; 146(6):703-721.
25. Qu N, Zhou XY, Han L, Wang L, Xu JX, Zhang T, et al. Combination of PPT with LiCl Treatment Prevented Bilateral Ovariectomy-Induced Hippocampal-Dependent Cognition Deficit in Rats. Mol Neurobiol 2016; 53(2):894-904.
26. Wang X, Liu D, Huang HZ, Wang ZH, Hou TY, Yang X, et al. A Novel MicroRNA-124/PTPN1 Signal Pathway Mediates Synaptic and Memory Deficits in Alzheimer's Disease. Biol Psychiatry 2018; 83(5):395-405.
27. Sulimai N, Lominadze D. Fibrinogen and Neuroinflammation During Traumatic Brain Injury. Mol Neurobiol 2020; 57(11):4692-4703.
28. Wang Q, Yu C, Shi S, Su X, Zhang J, Ding Y, et al. An analysis of plasma reveals proteins in the acute phase response pathway to be candidate diagnostic biomarkers for depression. Psychiatry Res 2019; 272:404-410.

29. Wang HY, Bakshi K, Frankfurt M, Stucky A, Goberdhan M, Shah SM, et al. Reducing amyloid-related Alzheimer's disease pathogenesis by a small molecule targeting filamin A. J Neurosci 2012; 32(29):9773-84.
30. Bryant CE, Spring DR, Gangloff M, Gay NJ. The molecular basis of the host response to lipopolysaccharide. Nat Rev Microbiol 2010; 8(1):8-14.
31. Pal D, Dasgupta S, Kundu R, Maitra S, Das G, Mukhopadhyay S, et al. Fetuin-A acts as an endogenous ligand of TLR4 to promote lipid-induced insulin resistance. Nat Med 2012; 18(8):1279-85.
32. Ramsey JM, Cooper JD, Bot M, Guest PC, Lamers F, Weickert CS, et al. Sex Differences in Serum Markers of Major Depressive Disorder in the Netherlands Study of Depression and Anxiety (NESDA). PLoS One 2016; 11(5):e0156624.
33. Huang SH, Chi F, Peng L, Bo T, Zhang B, Liu LQ, et al. Vimentin, a Novel NF-kappaB Regulator, Is Required for Meningitic Escherichia coli K1-Induced Pathogen Invasion and PMN Transmigration across the Blood-Brain Barrier. PLoS One 2016; 11(9):e0162641.
34. Amantea D, Nappi G, Bernardi G, Bagetta G, Corasaniti MT. Post-ischemic brain damage: pathophysiology and role of inflammatory mediators. FEBS J 2009; 276(1):13-26.
35. Zub E, Canet G, Garbelli R, Blaquiere M, Rossini L, Pastori C, et al. The GR-ANXA1 pathway is a pathological player and a candidate target in epilepsy. FASEB J 2019; 33(12):13998-14009.
36. Tu Y, Xie P, Du X, Fan L, Bao Z, Sun G, et al. S100A11 functions as novel oncogene in glioblastoma via S100A11/ANXA2/NF-kappaB positive feedback loop. J Cell Mol Med 2019; 23(10):6907-6918.
37. Sundblad V, Morosi LG, Geffner JR, Rabinovich GA. Galectin-1: A Jack-of-All-Trades in the Resolution of Acute and Chronic Inflammation. J Immunol 2017; 199(11):3721-3730.
38. Pregnolato S, Chakkarapani E, Isles AR, Luyt K. Glutamate Transport and Preterm Brain Injury. Front Physiol 2019; 10:417.
39. Lee DH, Seubert S, Huhn K, Brecht L, Rotger C, Waschbisch A, et al. Fingolimod effects in neuroinflammation: Regulation of astroglial glutamate transporters? PLoS One 2017; 12(3):e0171552.
40. Jatana M, Giri S, Ansari MA, Elango C, Singh AK, Singh I, et al. Inhibition of NF-kappaB activation by 5-lipoxygenase inhibitors protects brain against injury in a rat model of focal cerebral ischemia. Journal of neuroinflammation 2006; 3:12.
41. Liu CH, Tan YZ, Li DD, Tang SS, Wen XA, Long Y, et al. Zileuton ameliorates depressive-like behaviors, hippocampal neuroinflammation, apoptosis and synapse dysfunction in mice exposed to chronic mild stress. Int Immunopharmacol 2020; 78:105947.
42. Joshi YB, Giannopoulos PF, Chu J, Pratico D. Modulation of lipopolysaccharide-induced memory insult, gamma-secretase, and neuroinflammation in triple transgenic mice by 5-lipoxygenase. Neurobiol Aging 2014; 35(5):1024-31.
43. Jin JH, Ngoc TM, Bae K, Kim YS, Kim HP. Inhibition of experimental atopic dermatitis by rhubarb (rhizomes of Rheum tanguticum) and 5-lipoxygenase inhibition of its major constituent, emodin.

Phytother Res 2011; 25(5):755-9.

44. Duman RS, Aghajanian GK. Synaptic dysfunction in depression: potential therapeutic targets. Science 2012; 338(6103):68-72.
45. Kang HJ, Voleti B, Hajszan T, Rajkowska G, Stockmeier CA, Licznerski P, et al. Decreased expression of synapse-related genes and loss of synapses in major depressive disorder. Nat Med 2012; 18(9):1413-7.
46. Luo M, Jones SM, Peters-Golden M, Brock TG. Nuclear localization of 5-lipoxygenase as a determinant of leukotriene B4 synthetic capacity. Proceedings of the National Academy of Sciences of the United States of America 2003; 100(21):12165-70.
47. Yu BP, Chung HY. Adaptive mechanisms to oxidative stress during aging. Mechanisms of ageing and development 2006; 127(5):436-43.
48. Ahn KS, Aggarwal BB. Transcription factor NF-kappaB: a sensor for smoke and stress signals. Annals of the New York Academy of Sciences 2005; 1056:218-33.
49. Yirmiya R, Rimmerman N, Reshef R. Depression as a microglial disease. Trends Neurosci 2015; 38(10):637-58.
50. Kreisel T, Frank MG, Licht T, Reshef R, Ben-Menachem-Zidon O, Baratta MV, et al. Dynamic microglial alterations underlie stress-induced depressive-like behavior and suppressed neurogenesis. Mol Psychiatry 2014; 19(6):699-709.
51. Soltys Z, Ziaja M, Pawlinski R, Setkowicz Z, Janeczko K. Morphology of reactive microglia in the injured cerebral cortex. Fractal analysis and complementary quantitative methods. J Neurosci Res 2001; 63(1):90-7.
52. Yang SS, Lin L, Liu Y, Wang J, Chu J, Zhang T, et al. High Morphologic Plasticity of Microglia/Macrophages Following Experimental Intracerebral Hemorrhage in Rats. Int J Mol Sci 2016; 17(7):1181-93.
53. Duda P, Hajka D, Wojcicka O, Rakus D, Gizak A. GSK3beta: A Master Player in Depressive Disorder Pathogenesis and Treatment Responsiveness. Cells 2020; 9(3):127.
54. Joshi YB, Giannopoulos PF, Chu J, Sperow M, Kirby LG, Abood ME, et al. Absence of ALOX5 gene prevents stress-induced memory deficits, synaptic dysfunction and tauopathy in a mouse model of Alzheimer's disease. Hum Mol Genet 2014; 23(25):6894-902.
55. Bansal Y, Singh R, Parhar I, Kuhad A, Soga T. Quinolinic Acid and Nuclear Factor Erythroid 2-Related Factor 2 in Depression: Role in Neuroprogression. Front Pharmacol 2019; 10:452.
56. Rada P, Rojo AI, Chowdhry S, McMahon M, Hayes JD, Cuadrado A. SCF/{beta}-TrCP promotes glycogen synthase kinase 3-dependent degradation of the Nrf2 transcription factor in a Keap1-independent manner. Mol Cell Biol 2011; 31(6):1121-33.
57. Wu H, Kong L, Cheng Y, Zhang Z, Wang Y, Luo M, et al. Metallothionein plays a prominent role in the prevention of diabetic nephropathy by sulforaphane via up-regulation of Nrf2. Free Radic Biol Med 2015; 89:431-42.

58. Cuadrado A. Structural and functional characterization of Nrf2 degradation by glycogen synthase kinase 3/beta-TrCP. Free Radic Biol Med 2015; 88(Pt B):147-157.
59. Qu Y, Wu J, Chen D, Zhao F, Liu J, Yang C, et al. MiR-139-5p inhibits HGTD-P and regulates neuronal apoptosis induced by hypoxia-ischemia in neonatal rats. Neurobiol Dis 2014; 63:184-93.
60. Chen RJ, Kelly G, Sengupta A, Heydendael W, Nicholas B, Beltrami S, et al. MicroRNAs as biomarkers of resilience or vulnerability to stress. Neuroscience 2015; 305:36-48.
61. Morlet E, Hozer F, Costemale-Lacoste JF. Neuroprotective effects of lithium: what are the implications in humans with neurodegenerative disorders? Geriatr Psychol Neuropsychiatr Vieil 2018; 16(1):78-86.
62. Beurel E, Grieco SF, Jope RS. Glycogen synthase kinase-3 (GSK3): regulation, actions, and diseases. Pharmacol Ther 2015; 148:114-31.
63. Joshi YB, Giannopoulos PF, Chu J, Sperow M, Kirby LG, Abood ME, et al. Absence of ALOX5 gene prevents stress-induced memory deficits, synaptic dysfunction and tauopathy in a mouse model of Alzheimer's disease. Hum Mol Genet 2014; 23(25):6894-902.
64. Ramos-Gomez M, Kwak MK, Dolan PM, Itoh K, Yamamoto M, Talalay P, et al. Sensitivity to carcinogenesis is increased and chemoprotective efficacy of enzyme inducers is lost in nrf2 transcription factor-deficient mice. Proc Natl Acad Sci U S A 2001; 98(6):3410-5.
65. Zhang M, An C, Gao Y, Leak RK, Chen J, Zhang F. Emerging roles of Nrf2 and phase II antioxidant enzymes in neuroprotection. Prog Neurobiol 2013; 100:30-47.
66. Rojo AI, Innamorato NG, Martin-Moreno AM, De Ceballos ML, Yamamoto M, Cuadrado A. Nrf2 regulates microglial dynamics and neuroinflammation in experimental Parkinson's disease. Glia 2010; 58(5):588-98.
67. Martin-de-Saavedra MD, Budni J, Cunha MP, Gomez-Rangel V, Lorrio S, Del BL, et al. Nrf2 participates in depressive disorders through an anti-inflammatory mechanism. Psychoneuroendocrinology 2013; 38(10):2010-22.
68. McMahon M, Thomas N, Itoh K, Yamamoto M, Hayes JD. Dimerization of substrate adaptors can facilitate cullin-mediated ubiquitylation of proteins by a "tethering" mechanism: a two-site interaction model for the Nrf2-Keap1 complex. J Biol Chem 2006; 281(34):24756-68.
69. Lee SY, Lee SJ, Han C, Patkar AA, Masand PS, Pae CU. Oxidative/nitrosative stress and antidepressants: targets for novel antidepressants. Prog Neuropsychopharmacol Biol Psychiatry 2013; 46:224-35.
70. Li W, Kong AN. Molecular mechanisms of Nrf2-mediated antioxidant response. Mol Carcinog 2009; 48(2):91-104.
71. Park SY, Jin ML, Ko MJ, Park G, Choi YW. Anti-neuroinflammatory Effect of Emodin in LPS-Stimulated Microglia: Involvement of AMPK/Nrf2 Activation. Neurochem Res 2016; 41(11):2981-2992.
72. Gu JW, Hasuo H, Takeya M, Akasu T. Effects of emodin on synaptic transmission in rat hippocampal CA1 pyramidal neurons in vitro. Neuropharmacology 2005; 49(1):103-11.

73. Taler M, Aronovich R, Henry HS, Dar S, Sasson E, Weizman A, et al. Regulatory effect of lithium on hippocampal blood-brain barrier integrity in a rat model of depressive-like behavior. Bipolar Disord 2021; 23(1):55-65.
74. Lopez-Lopez AL, Jaime HB, Escobar VM, Padilla MB, Palacios GV, Aguilar F. Chronic unpredictable mild stress generates oxidative stress and systemic inflammation in rats. Physiol Behav 2016; 161:15-23.
75. Lu XT, Liu YF, Zhao L, Li WJ, Yang RX, Yan FF, et al. Chronic psychological stress induces vascular inflammation in rabbits. Stress 2013; 16(1):87-98.
76. Uz T, Dimitrijevic N, Imbesi M, Manev H, Manev R. Effects of MK-886, a 5-lipoxygenase activating protein (FLAP) inhibitor, and 5-lipoxygenase deficiency on the forced swimming behavior of mice. Neurosci Lett 2008; 436(2):269-72.
77. Luo Y, Kuang S, Xue L, Yang J. The mechanism of 5-lipoxygenase in the impairment of learning and memory in rats subjected to chronic unpredictable mild stress. Physiol Behav 2016; 167:145-153.
78. Ford-Hutchinson AW, Gresser M, Young RN. 5-Lipoxygenase. Annu Rev Biochem 1994; 63:383-417.
79. Wu L, Miao S, Zou LB, Wu P, Hao H, Tang K, et al. Lipoxin A4 inhibits 5-lipoxygenase translocation and leukotrienes biosynthesis to exert a neuroprotective effect in cerebral ischemia/reperfusion injury. J Mol Neurosci 2012; 48(1):185-200.

Table

Table 1 Antibodies used in this study

Antibody	Epitopes	mAb/pAb	WB	IHC or IF	Source
DM1A	alpha-tublin	mAb	1:2000		Abcam
ba1	ionized calcium binding adapter molecule 1	pAb		1:200	Wako
-GSK-3β	total GSK-3β	pAb	1:1000		Cell Signaling
p-GSK-3β	p-GSK-3β at Ser9	pAb	1:1000		Cell Signaling
-Nrf2	total Nrf2	pAb	1:500		Abcam
p-Nrf2	p-Nrf2 at Ser40	pAb	1:1000	1:100	Abcam
5-LO	total 5 Lipoxygenase	mAb	1:1000	1:100	Abcam
NF-κB p65	total NF-κB p65	mAb	1:500		Cell Signaling
GAPDH	full length GAPDH	MAb	1:1000		Abcam
Histone3	total histone H3 protein	pAb	1:1000		Cell Signaling

p, phosphorylated; mAb, monoclonal antibody; pAb, polyclonal antibody;WB, western blotting; IHC, immunohistochemistry; IF, Immunofluorescence.

Figures

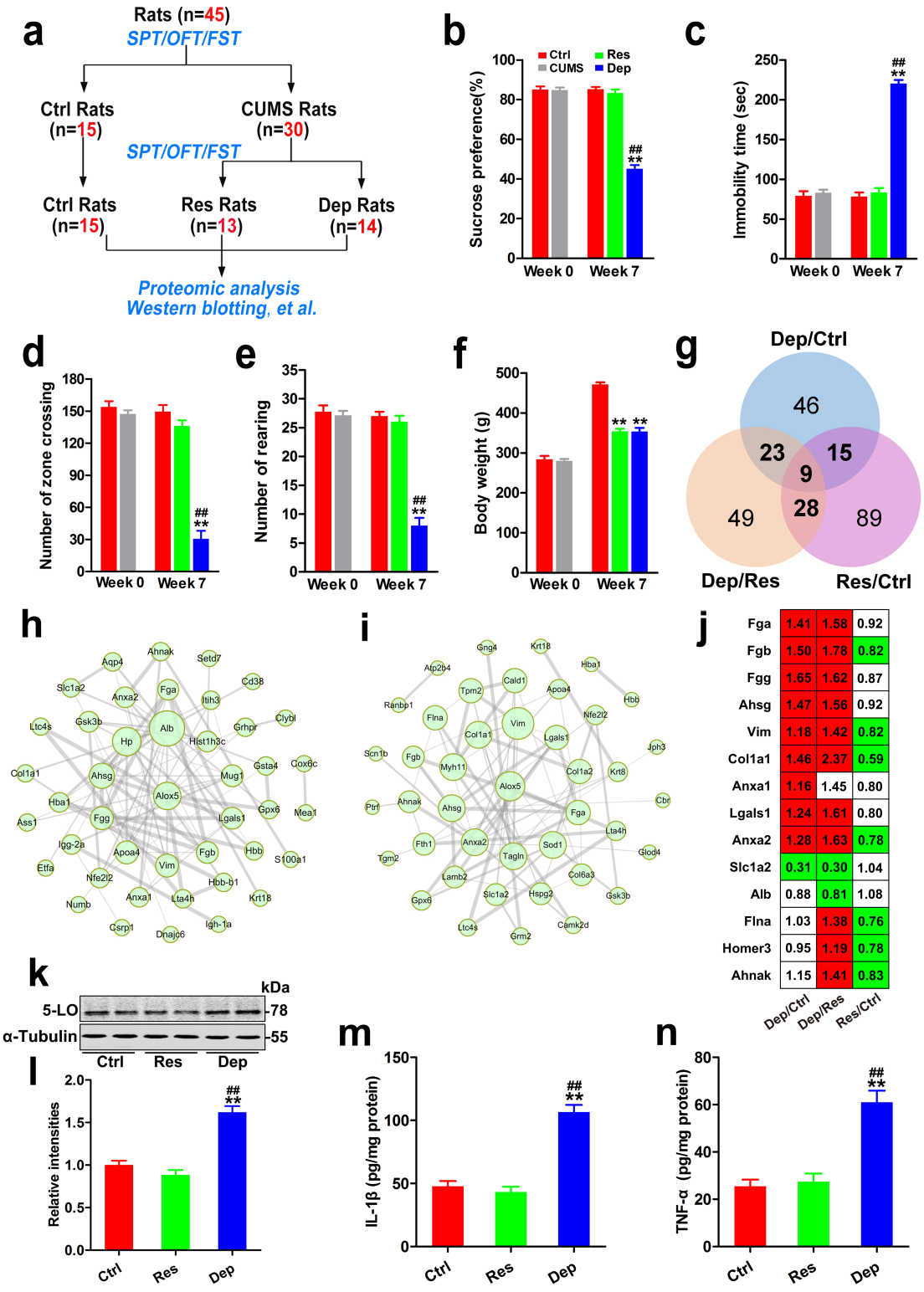

Figure 1

Inflammation with increased 5-lipoxygenase (5-LO) was found in hippocampus of Dep rats. (a) Schematic illustration of the first part of this research. 45 rats were evaluated by sucrose preference test (SPT), forced swimming test (FST) and open field test (OFT). Then, 15 rats were randomly chosen as control (Ctrl) rats, and 30 rats were daily exposed to chronic unpredicted mild stress (CUMS). After 7 weeks' CUMS exposure, 13 depression resistant (Res) rats and 14 depression (Dep) rats were obtained by

SPT, SPT and OFT. The other 3 rats did not fit either group. The hippocampi were extracted and investigated by isobaric tags for relative and absolute quantitation (iTRAQ) (n=3/group). The sucrose preference rates in SPT (b), immobility time in FST (c), numbers of zone crossing (d) and rearing times (e) in OFT, and the body weights of rats (f) were recorded. 259 differentially expressed proteins were obtained, e.g. 93 differentially expressed proteins in Dep/Ctrl, 109 differentially expressed proteins in Dep/Res, and 141 differentially expressed proteins in Res/Ctrl (g). By STRING 11.0 (https://string-db.org/), protein-protein interaction (PPI) networks construction for differentially expressed proteins in Dep/Ctrl rats (h) and Dep/Res rats (i) were qualified. The thickness of edges was decided by the combined score. The differentially expressed proteins tightly related to inflammation were listed with a ratio (j, red color means significantly up-regulated and green color means significantly down-regulated). Hippocampal levels of 5-LO (k, l), interleukin-1β (IL-1β, m) and tumor necrosis factor-α (TNF-α, n) in Ctrl, Res, and Dep rats were tested by Western blotting (k, l, n=6/group) and ELISA (m, n, n=3 /group). Data were analyzed by one-way ANOVA and expressed as the mean ± SEM, ** p <0.01 Res or Dep versus Ctrl. ## p <0.01 Dep versus Res.

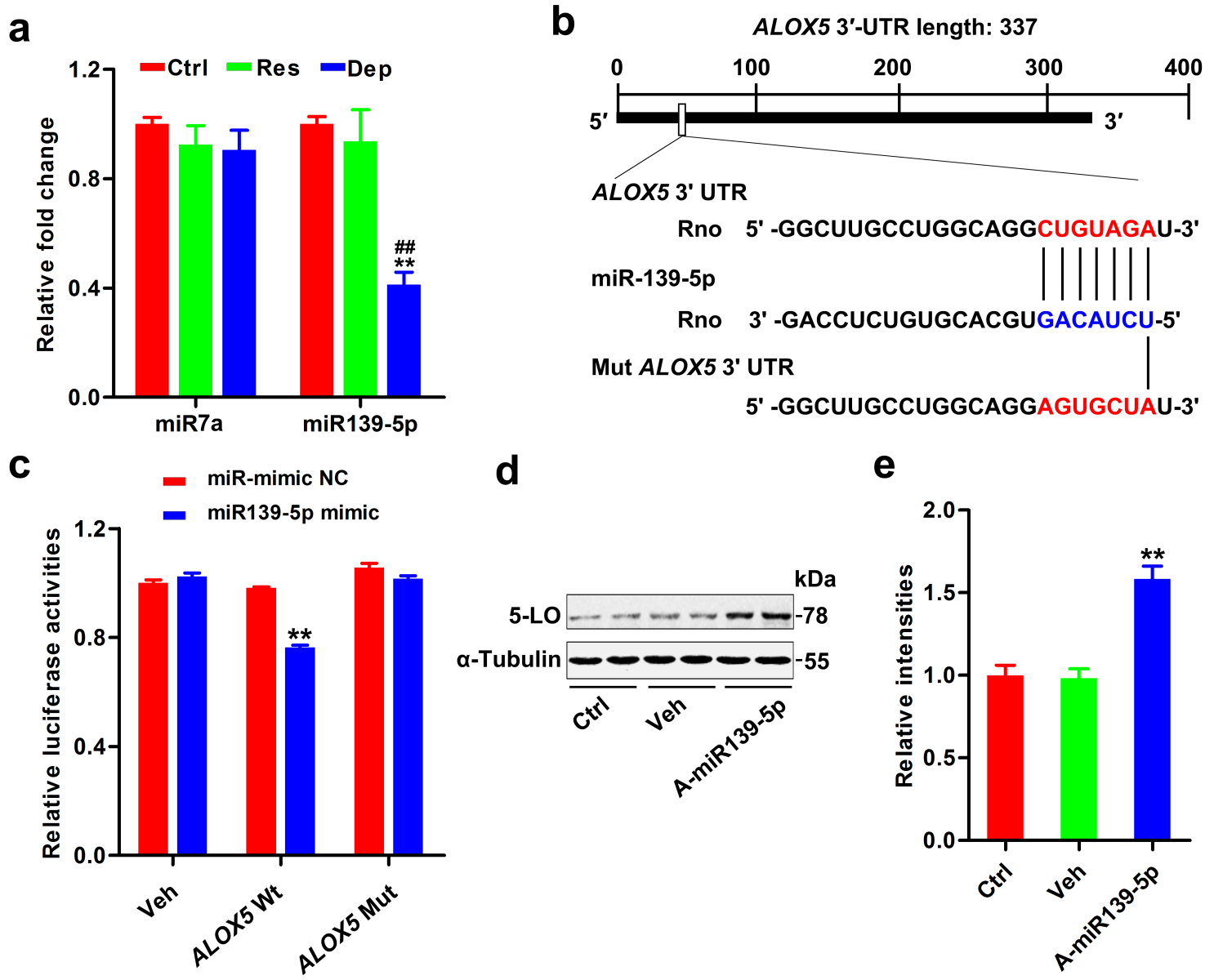

Figure 2

Down-regulation of miR139-5p was responsible for 5-LO elevation. Alterations in predicted miRNAs that target 5-LO in the hippocampus of CUMS-exposed rats (a, n=3 brains/group). ** p <0.01 Res or Dep versus Ctrl. ## p <0.01 Dep versus Res. The binding site for miR139-5p seed sequence in the ALOX5 3'-UTR (b). Luciferase reporter assay results demonstrated that miR139-5p targets ALOX5 3'-UTR (c). ** p<0.01 miR139-5p mimic versus the negative control-treated group (miR mimic NC). The 5-LO level in N2a cells treated with miR139-5p inhibitor (A-miR139-5p) or its scrambled control (Veh) was tested by Western blotting (d) and quantitatively analyzed (e). ** p<0.01 A-miR139-5p versus Veh. Data were analyzed by one-way ANOVA and presented as mean ± S.E.M..

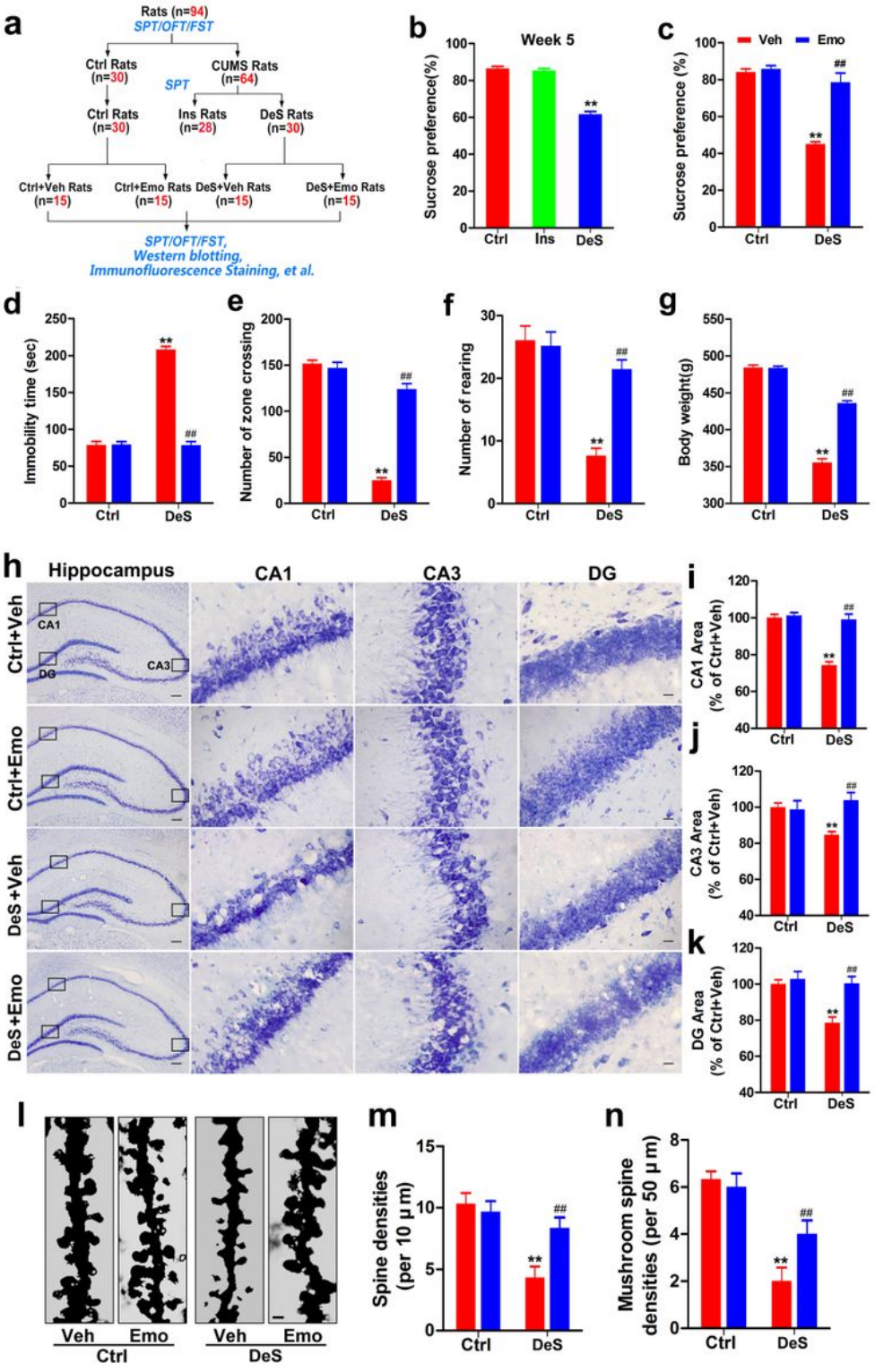

Figure 3

Emodin ameliorated depression-like behaviors in DeS rats. Schematic illustration of the second part of this research (a). Sucrose preference test (SPT), forced swimming test (FST) and open field test (OFT) were performed as shown. By the percentage of sucrose water preference in SPT, we selected out 30 depression-susceptible rats (DeS rats) and 28 stress insensitive rats (Ins rats) from 64 rats at the end of 5th week (b). 30 rats unstressed were used as control (Ctrl). Then, 2 weeks' treatment of emodin (Emo)

(80mg/kg/day, intragastric administration) or the same volume of solvent (Veh, intragastric administration) were performed in DeS and Ctrl rats. Simultaneously, Emo treated DeS rats (DeS+Emo) and Veh treated DeS rats (DeS+Veh) were also exposed to CUMS. After these processes, the sucrose preference rates in SPT (c), immobility time in FST (d), numbers of zone crossing (e) and rearing times (f) in OFT, and the body weights (g) were recorded (n=15/group). Hippocampal neurons were shown by Nissl staining (h, left scale bar=200 μm, right scale bar=20 μm) and quantified in CA1 (i), CA3 (j) and DG (k) regions (n=3 brains/group). The black rectangle regions in the left panels are shown in higher magnification in the right panels. The dendrites of the CA1 neurons were shown by Golgi staining (l, n=3 brains/group, scale bar=1 μm). Quantification of the density of dendritic spine (m) and mushroom-type spine (n) were calculated by Image-Pro Plus 6.0 software (n=21 dendrites from 3 brains/group). Data were analyzed by one-way ANOVA and presented as mean ± S.E.M., ** $p<0.01$ DeS+Veh versus Ctrl+Veh, ## $p<0.01$ DeS+Emo versus DeS+Veh.

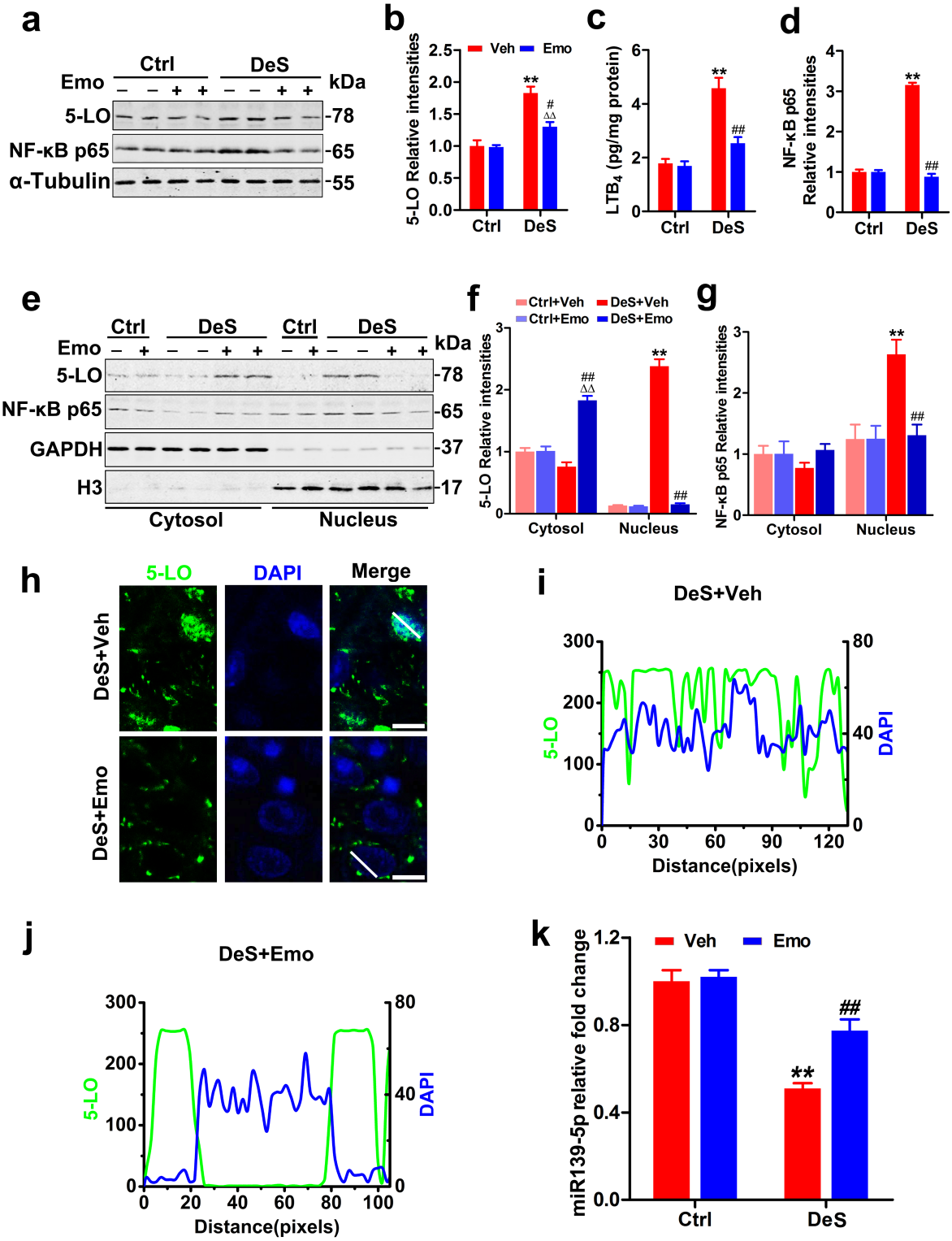

Figure 4

Emodin inhibited the activation of 5-LO and nuclear factor-κB (NF-κB)by up-regulating miR-139-5p. Hippocampal levels of 5-LO and activated NF-κB (NF-κB p65) were tested by Western blotting (a) and quantitative analysis (b, d) (n=6 brains/group). By ELISA, hippocampal levels of leukotriene B4 (LTB4) were assessed (c, n=3 brains/group). The levels of 5-LO and NF-κB p65 in the nuclear and cytoplasmic fractions were detected by Western blotting (e) and quantitative analysis (f, g) (n=6 brains/group). By

immunofluorescence staining (h, scale bar=20 μm, n=3 brains/group) and fluorescence intensity detection at the same location (i, j, the quantified areas were defined by white lines), the significant co-localization between 5-LO (green) and DAPI (blue, marking nucleus) was shown in the hippocampal CA1 of DeS+Veh rats, and 5-LO was transferred from the nucleus to the cytoplasm by emodin. Hippocampal miR139-5p was analyzed by quantitative real-time PCR (k, n=3 brains/group). Data were analyzed by one-way ANOVA and presented as mean ± S.E.M., ** p<0.01 DeS+Veh versus Ctrl+Veh, ΔΔ p<0.01 DeS+Emo versus Ctrl+Emo, # p<0.05, ## p<0.01 DeS+Emo versus DeS+Veh.

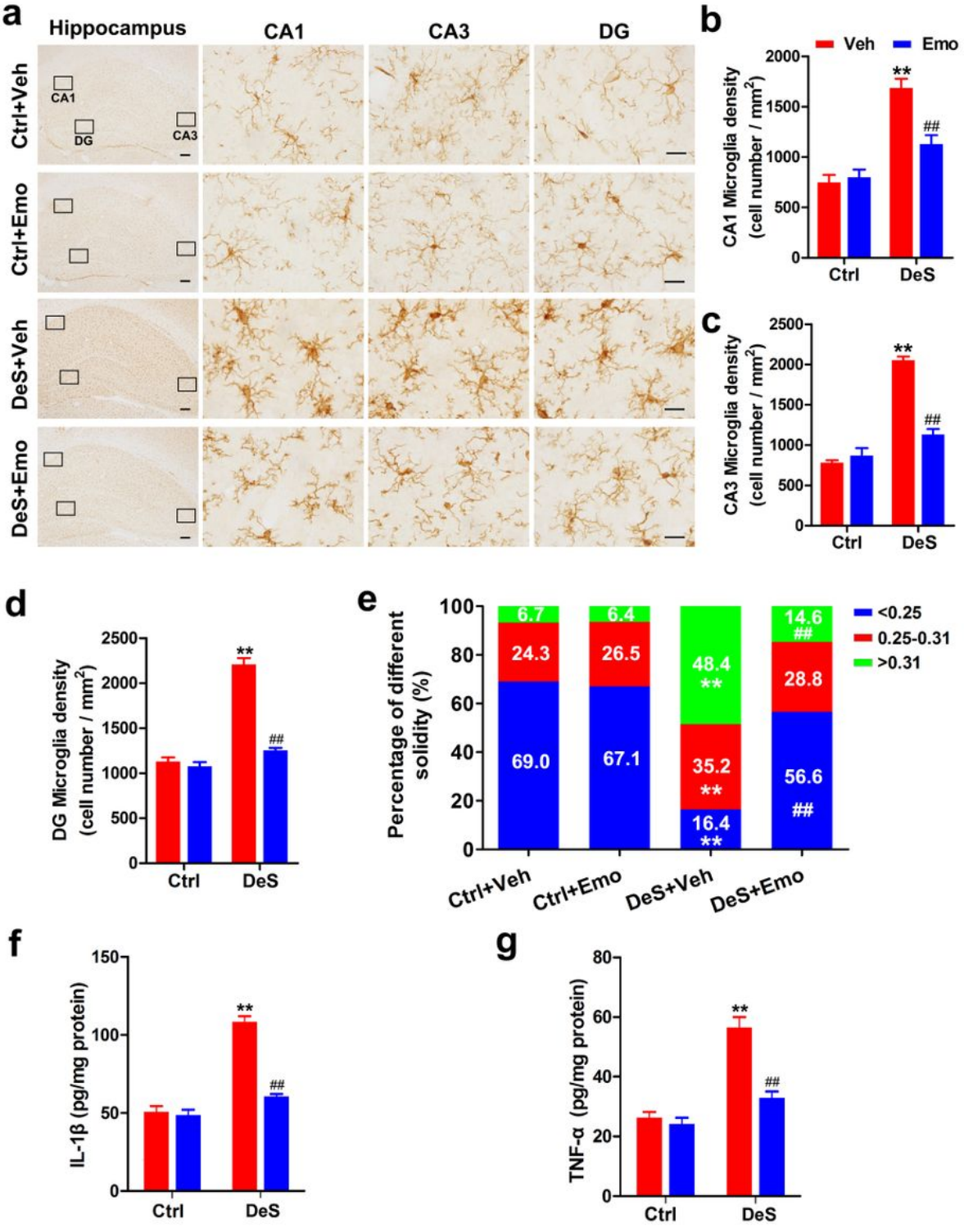

Figure 5

Depression associated microglia activation was inhibited by emodin. By immunohistochemistry staining with Iba1 (a marker of microglia), hippocampal microglia were shown (a) (left scale bar=200 μm, right scale bar=20 μm). The black rectangle regions in the left panels are shown in higher magnification in the right panels. The densities of microglia in CA1 (b), CA3 (c) and DG (d) regions were calculated (n=3 brains/group). The solidity value analysis was used to evaluate the activation of microglia. Higher solidity value indicates higher activity of microglia. We divided the solidity value of the microglia into 3 grades (<0.25, 0.25–0.31, >0.31), and the percentages of microglia with different grades in different groups were shown in (e, n=3 brains/group). By ELISA, hippocalpal levels of interleukin-1β (IL-1β, f) and tumor necrosis factor-α (TNF-α, g) were assessed (n=3 brains/group). Data were analyzed by one-way ANOVA and presented as mean ± S.E.M., ** p<0.01 DeS+Veh versus Ctrl+Veh, ## p<0.01 DeS+Emo versus DeS+Veh.

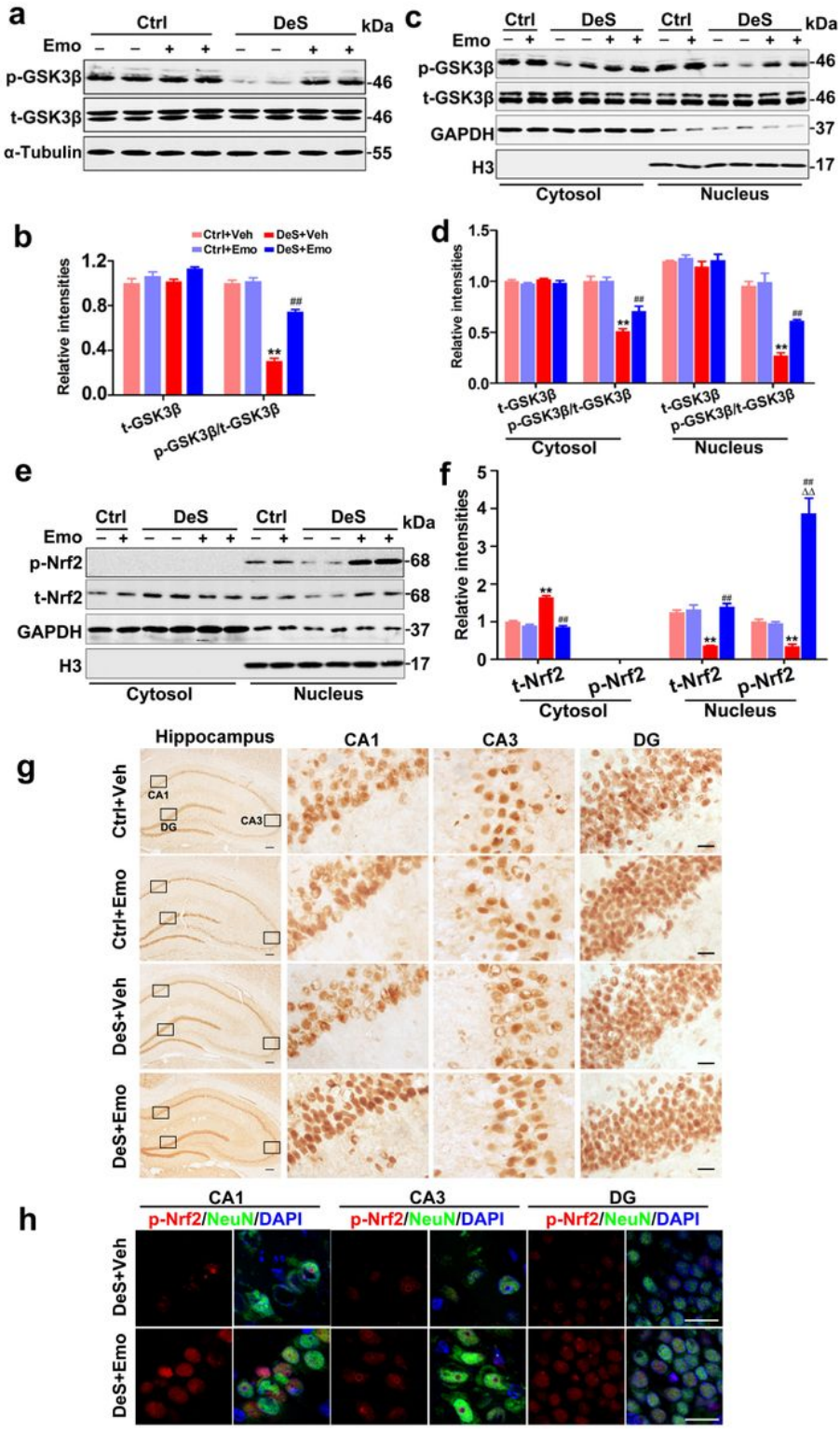

Figure 6

Emodin inhibited hippocampal GSK3β activation. Levels of hippocampal total GSK3β (t-GSK3β) and phosphorylated GSK3β (p-GSK3β, Ser9) were shown by Western blotting (a) and quantitatively analyzed (b, n=6 brains/group). Meanwhile, the levels of t-GSK3β and p-GSK3β in the nuclear and cytoplasmic fractions were tested by Western blotting (c) and quantitatively analyzed (d, n=6 brains/group). The levels of total nuclear factor erythroid 2-related factor 2 (t-Nrf2) and phosphorylated Nrf2 at Ser40 (p-Nrf2) in

the nuclear and cytoplasmic fractions were tested by Western blotting (e) and quantitatively analyzed (f, n=6 brains/group). Data were analyzed by one-way ANOVA and presented as mean ± S.E.M., ** p<0.01 DeS+Veh versus Ctrl+Veh, ΔΔ p<0.01 DeS+Emo versus Ctrl+Emo, ## p<0.01 DeS+Emo versus DeS+Veh. By immunohistochemistry staining (g), phosphorylated Nrf2 at Ser40 (p-Nrf2) positive hippocampal neurons were shown (left scale bar=200 μm, right scale bar=20 μm, n=3 brains/group). The black rectangle regions in the left panels are shown in higher magnification in the right panels. By double-label immunofluorescence staining (h), compared with DeS+Veh rats, more p-Nrf2 (red) positive cells in DeS+Emo rats were shown NeuN (a marker of neuron, green) positive, and more p-Nrf2 staining co-localized with DAPI in DeS+Emo rats (blue, marking nucleus) (scale bar=20 μm, n=3 brains/group).

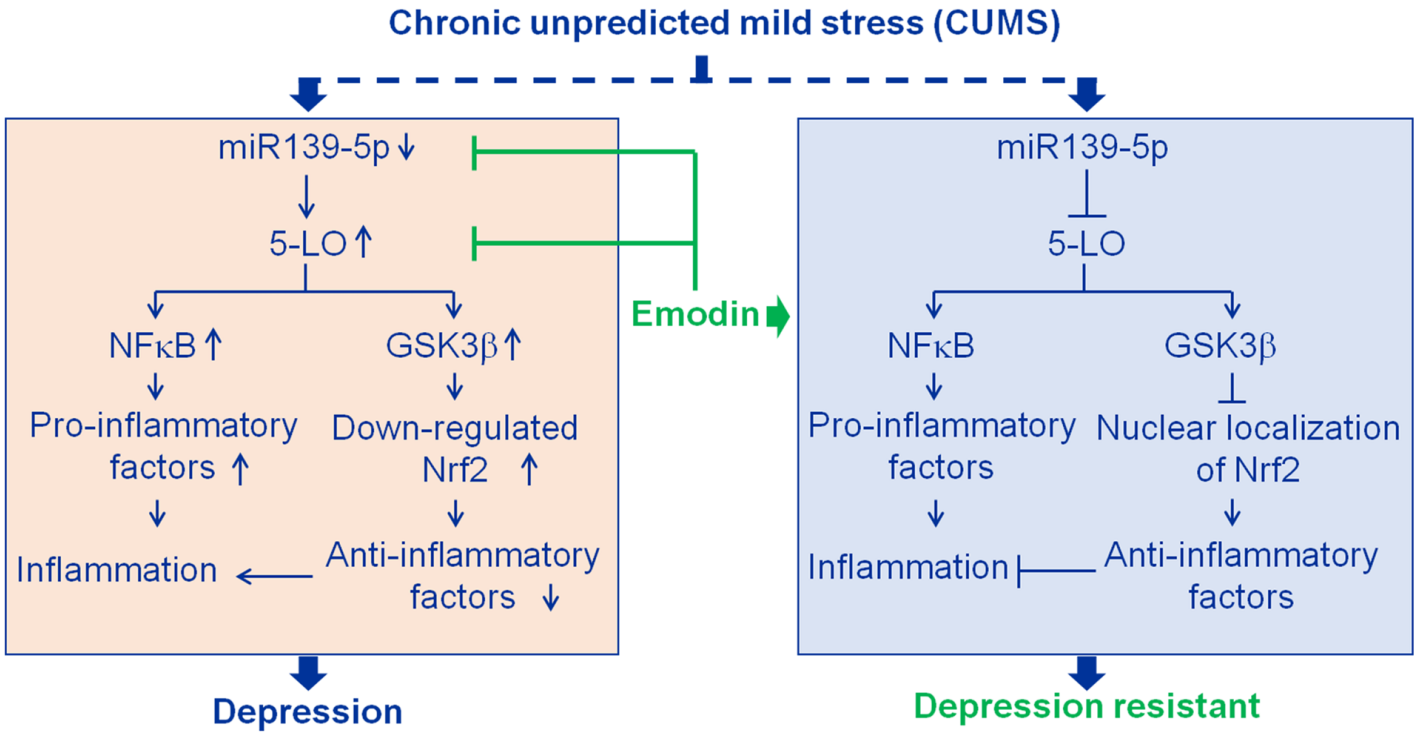

Figure 7

Results summary diagram. Hippocampal inflammation plays an important role in depression. Emodin prevented chronic unpredicted mild stress (CUMS)-induced depression mainly by targeting miR139-5p/5-lipoxygenase (5-LO). Nuclear factor-κB (NF-κB) and glycogen synthase kinase 3β (GSK3β) are the downstream factors of 5-LO. Nuclear factor erythroid 2-related factor 2 (Nrf2), a transcriptional activator of antioxidant genes, down-regulated by activated GSK3β.